Regenerative Therapy 20 (2022) 32–40

Contents lists available at ScienceDirect

Regenerative Therapy

journal homepage: http://www.elsevier.com/locate/reth

Original Article

MiRNA-320a-5p contributes to the homeostasis of osteogenesis and adipogenesis in bone marrow mesenchymal stem cell

Ying Zhang [a, b, 1], Ning Zhang [c, 1], Qiushi Wei [d, e], Yipping Dong [f], Youwen Liu [a], Qiang Yuan [f], Wei He [d, e], Zhenhao Jing [f], Zhinan Hong [d, e], Leilei Zhang [a], Haibin Wang [b, **], Wuyin Li [a, *]

[a] Medical Center of Hip, Luoyang Orthopedic-Traumatological Hospital (Orthopedics Hospital of Henan Province), Luoyang, Henan, 471002, PR China
[b] Guangzhou University of Traditional Chinese Medicine, Guangzhou, Guangdong, 510405, PR China
[c] Hunan University of Traditional Chinese Medicine, Changsha, Hunan, 410208, PR China
[d] Institute of Orthopaedics of Guangzhou University of Traditional Chinese Medicine, Guangzhou, 510240, PR China
[e] The Third Affiliated Hospital of Guangzhou University of Traditional Chinese Medicine, Guangzhou, 510240, PR China
[f] Henan University of Traditional Chinese Medicine, Zhengzhou, Henan, 450046, PR China

ARTICLE INFO

Article history:
Received 26 July 2021
Received in revised form
19 January 2022
Accepted 2 March 2022

Keywords:
TIONFH
miRNA-320a
RUNX2
Osteoblast differentiation
Adipocyte differentiation

ABSTRACT

Objective: A number of miRNAs and their targets were dragged in the differentiation of bone marrow mesenchymal stem cells (BMSCs). We aimed to elaborate the underlying molecular mechanisms of miRNA-320a in the osteoblast and adipocyte differentiation.
Methods: Trauma-induced osteonecrosis of the femoral head (TIONFH) and normal control samples (n = 10 for each group) were collected, followed by miRNA chip analysis to identify the differentially expressed miRNAs. H&E staining was used to observe the pathological development of TIONFH. Lentiviral vector was used for overexpression and inhibition of miRNA-320a in vitro. Quantitative real-time PCR (qPCR), Western blotting and immunohistochemistry staining were employed to determine the expression of interested genes at mRNA or protein level. Luciferase report assay was employed to determine the binding of miRNA-320a and RUNX2. Alkaline phosphatase (ALP) and Alizarin red staining were performed to observe the osteogenesis and Oil red O staining were conducted to visualize the adipogenesis.
Results: Expression of miRNA-320a was up-regulated while RUNX2 expression was down-regulated in TIONFH than Normal control. Luciferase report assay confirmed that miRNA-320a directly targeted to the 3′UTR of RUNX2. miRNA-320a overexpression significantly declined the expressions of osteogenesis-related markers: RUNX2, OSTERIX, Collagen I, Osteocalcin and Osteopontin. ALP and Alizarin red staining confirmed the inhibition function of miRNA-320a in osteogenesis of BMSCs. miRNA-320a inhibition significantly decreased the expression of adipogenesis-related markers: AP2, C/EBPα, FABP4 and PPARγ. Oil Red O staining confirmed the miRNA-320a inhibition reduced adipogenesis of BMSCs.
Conclusions: miRNA-320a inhibits osteoblast differentiation via targeting RUNX2 and promotes adipocyte differentiation of BMSCs.

1. Introduction

Osteonecrosis of the femoral head (ONFH) is a widespread and intractable disease, which is responsible for about 8–12% of all total hip arthroplasty (THA) cases in America [1]. Various factors were implicated to ONFH, dominated by alcoholism and corticosteroid use [2,3]. According to the aetiological factors, ONFH can categorized into two major groups, including trauma-induced ONFH

* Corresponding author. Medical Center of Hip, Luoyang Orthopedic-Traumatological Hospital (Orthopedics Hospital of Henan Province), No. 82 Qiming South Road, Luoyang, Henan, 471002, PR China.
** Corresponding author.
E-mail addresses: hipknee@163.com (H. Wang), liwuyin2000@163.com (W. Li).
Peer review under responsibility of the Japanese Society for Regenerative Medicine.
[1] Contributed equally to this work.

https://doi.org/10.1016/j.reth.2022.03.001

(TIONFH) and nontraumatic ONFH [4]. ONFH ultimately progressed to collapse of the femoral head, which is generally treated with THA [5]. As the most significant complications, collapse of the femoral head also resulted in insufferable symptoms like severe pain, claudication, and clinical abalienation [6,7]. Moreover, the femoral head collapse usually led to hip osteoarthritis (OA), its pain would worsen over time [6,8]. In brief, ONFH results in inestimable loss of labor worldwide because of its disabling properties [9].

Due to the marrow fat deposition would result in the ischemia of blood sinusoid in compartmental bone, the lipid deposition was dragged in the development of ONFH [10–12]. Further studies suggested that the marrow fat accumulation was caused by the adipogenesis of bone marrow mesenchymal stem cells (BMSCs) [13–15]. BMSCs possess the differentiation capacity to various cells, such as adipocytes and osteoblasts [16–19]. Sheng et al. demonstrated that the development of ONFH was close associated with the elevated adipogenesis of BMSCs on the rabbit model [10]. The dysfunction of BMSCs was demonstrated to be involved in the progression of the ONFH patients, including elevated adipogenesis, compromised osteogenesis, impaired proliferation ability, and elevated apoptosis [20,21]. Additionally, the abnormal gene expression was considered as the crucial agent of the dysfunction of BMSCs, especially in the homeostasis disruption of adipogenesis and osteogenesis [22].

Recently, the regulation of gene expression in ONFH cases has caused increasing attention [23]. Extensive studies mainly focused on investigating the biological function of microRNAs (miRNAs/miRs), which is a small single-strand non-coding RNA molecule (composed of approximately 22 nucleotides) [24,25]. miRNA is complementary to a segment of one or more message RNAs (mRNAs) and functions as the regulator of the corresponding gene [26,27]. A number of miRNAs and their targets were identified to involve in the regulation of BMSCs differentiation. For instance, miRNA-199b-5p was demonstrated to facilitate the osteogenesis of BMSCs via inhibition of glycogen synthase kinase-3β/β-catenin signaling pathway [28]. miRNA3a was proved to suppress the osteogenesis of BMSCs via targeting low-density lipoprotein-receptor-related protein 5 (LRP5) [29]. miRNA-99a was identified to inhibit the osteogenic differentiation via modulating the histone demethylase level of lysine (K)-specific demethylase 6B (KDM6B) [30]. Taken together, miRNAs and their targets play indispensable roles in the development of ONFH via controlling the homeostasis of adipogenesis and osteogenesis.

Our previous study had revealed that various miRNAs differentially expressed in TIONFH based on miRNAs expression profile analysis, and further experiments suggested that miRNA-93-5p mediated osteogenic differentiation by targeting morphogenetic protein-2 [31]. Of which, miRNA-320a also differentially expressed in TIONFH, but its roles in the development of TIONFH had not been investigated. Here, we proved that miRNA-320a inhibits the osteogenesis and promotes the adipogenesis of BMSCs. Our current study provides a reference for the future research on the molecular mechanism of BMSCs differentiation, and a potential target for the diagnosis and therapy of TIONFH.

2. Materials and methods

2.1. Patients and sample collection

TIONFH and normal control samples were selected from the femoral neck fractures patients who were treated with manual reduction and percutaneous cannulated screw fixation in the Henan Orthopaedic Hospital from January to April in 2015. Patients with femoral head necrosis after surgery were included in the TIONFH group (n = 10), and patients without femoral head necrosis more than 2 years after surgery were included in the Normal group (n = 10). The basic information of the included subjects listed in Table 1. This study was in consistent with the relevant provisions of the 1964 Helsinki Declaration and was permitted by the ethics committee of Henan Orthopaedic Hospital. Informed consent was acquired from all participants.

Venous blood blood was collected from each of the 20 participants with BD Vacutainer® blood collection tubes (BD, USA). The entire blood was placed at room temperature for 30 min and subsequently centrifuged (1800×*g*, 5 min) for separating serum. The acquired serum was aliquoted into microtubes and frozed with liquid nitrogen immediately. All serum samples were stored at −150 °C refrigerator (Thermo Fisher Scientific, USA) for following assays.

2.2. RNA isolation

Total RNA (including miRNA) was isolated by using TRIzol as the manual described. Subsequently, the RNasey Mini Kit (QIAGEN, Germany) were used to purify the obtained RNA. The quantity and quality of isolated RNA was examined using the NanoDrop™ 1000 spectrophotometer (Thermo Fisher Scientific, USA) and the integrity of RNA was confirmed by RNA gel electrophoresis.

2.3. qRT-PCR

The reverse transcription (RT) of miRNA was performed using the Bulge-Loop™ miRNA qRT-PCR kit as the manual described (RIBOBIO, China). The Mir-X miRNA qRT-PCR TB Green® Kit was used for following quantitative PCR (qPCR) assay as the manual described. The PCR procedure was performed on the Applied Biosystems 7500 Real-Time PCR system (Applied Biosystems, USA). The U6 non-coding small nuclear RNA (U6 snRNA) was used as the reference and the primers used for RT and qRT-PCR were listed in Table S1.

2.4. H&E staining

To observe the pathological development of the femoral head, we conducted the Hematoxylin & eosin (H&E) staining. In brief, samples were decalcified with EDTA firstly. Then the graded alcohol solutions were used for dehydration and the paraffin (Solarbio, China) was used to embed the samples. Next, the samples were cut into 4-μm slides with serial sections. Following H&E staining was conducted using the H&E staining kit (Solarbio, China) as the manual described.

2.5. Immumohistochemical (IHC) staining

To compare the differential expression of RUNX2 protein between the ONFH patients and NC, IHC staining was performed. After pretreatment, the samples were cut into 6-μm slides with serial sections. Firstly, the slides were treated with 0.25% trypsin (Solarbio, China) for repairing antigen, and then sealed tissue with 3% bull serum albumin (Servicebio, China) for 30 min. Next, the slides were incubated with the RUNX2 primary antibody (1:500,

Table 1
Basic information of the included subjects.

	TIONFH group (n = 10)	Normal group (n = 10)
Median age,range (years)	43 (20 ± 55)	45.745 (36 ± 57)
Sex		
Male (n)	5	9
Female (n)	5	1
Body mass index	24.08 ± 3.31	23.97 ± 3.65
Harris hip score	78.70 ± 13.77	93.10 ± 5.40
Visual analogue score	1.70 ± 1.49	0.30 ± 0.48

TIONFH, Trauma-induced osteonecrosis of the femoral head.

catalog no. sc-390351, Santa Cruz Biotechnology, USA) overnight. Then the slides were incubated with HRP secondary antibody (Servicebio, China) for 1 h. The EliVision™ plus kit (Maixin Biotechnologies, China) was used to visualize the antibody labelling. Diaminobenzidine (DAB) solution was added and incubated for 2 h at room temperature, and then were counterstained with hematoxylin, rinsed, air-dried. Lastly, neutralresinsize was used to seal the slides. The slides were examined under an Olympus® CX31 microscope (Tokyo, Japan) and were analyzed using ImageJ software (Scion Corp., USA) to calculated the area of positive staining and tissue area. The percentage of positive expression was defined as area of positive staining/area of tissue.

2.6. Cell culture, plasmids construction, and cell transfection

OriCell® human MSCs (Cyagen Biosciences, China) were purchased for the evaluation of differentiation ability and were cultured as the manual described. Briefly, the low glucose DMEM (Gibco, USA) with supplementation of 10% fetal bovine serum (FBS) (Invitrogen, USA) and 100 units/mL penicillin and streptomycin (Invitrogen, USA) were used for hMSCs incubation. Culture medium were replaced every 48−72 h and 0.25% trypsin (Solarbio, China) were used for detachment.

The lentivirus (LV) expression system was used to modulate the expression of miRNA-320a, which composed of three plasmids, PLVX-IRES-PURO/PLKO for insertions, psPAX2 for package, and pMD2. G for envelop. The sequence of mature miRNA-320a (5′-AAAAGCUGGGUUGAGAGGGCGA-3′) was downloaded from the miRbase database (http://www.mirbase.org/). The inhibitor sequence of miRNA-320a (5′-TCGCCCTCTCAACCCAGCTTTT-3′) was inserted into the PLVX-IRES-PURO plasmid. The PLKO plasmid was utilized for the overexpression of miRNA-320a. The full-length pre-has-miRNA-320a was synthesized (Sangon Biotech, China). Firstly, the PLVX-IRES-PURO plasmid and the inhibitor sequence were digested with XhoI and NotI (New England Biolabs, UK) and the PLKO plasmid and pre-has-miRNA-320a were digested with AgeI and EcoRI (New England Biolabs, UK). The acquired linear DNA fragments were purified and then ligated with the help of T4 ligase kit (Thermo Fisher Scientific, USA), respectively.

The lentivirus particles were generated by transfecting 293T cells with plasmids, psPAX2 and pMD2. G (Plasmids, psPAX2 and pMD2. G = 2:1:2) using lipo3000 (Invitrogen, USA). Following 48 h for transfecting, lentivirus particles was generated. BMSCs were cultured in Opti-MEM medium (Gibco, USA). For lentivirus particles transfection, BMSCs were seeded into 6-well plates with a concentration of 4×10^5 cells/well, and lentivirus particles were added to each well. Then, BMSCs were incubated at 37 °C with 5% CO^2. After 24 h of transduction, the medium was changed. The stable cell lines were constructed by adding 5 μg/mL of puromycin at 48 h after transduction.

2.7. Luciferase reporter assays

The wild and mutant 3′-UTR sequence of RUNX2 was synthesized and inserted into the Psicheck2.0 plasmid. Next, miRNA-320a NC/mimic and wild/mutant RUNX2 3′-UTR were co-transfected into the human embryonic kidney 293 (HEK 293) cells. The transfected cells were harvested at 24 h. And then the Firefly Luciferase Reporter Gene Assay Kit (Beyotime, China) was used to detect the activity of luciferase.

2.8. Alkaline phosphatase (ALP) and Alizarin red staining

To investigate the exact effect of miRNA-320a in the osteoblast differentiation of BMSCs, ALP and Alizarin red staining were performed. Firstly, the osteogenesis of BMSCs were induced by the osteogenic medium, which was composed of low glucose DMEM, 10% FBS, 100 mM/L dexamethasone, 50 uM/L 2-Phospho-L-ascorbic acid trisodium salt, 10 mM/L β-glycerophosphate (Gibco, USA). The LV expression system was utilized to overexpress the miRNA-320a with the control of the empty LV. For ALP staining, the cell samples were collected at 7 days and washed with PBS twice, then fixed by using 4% polyoxymethylene at 10 min. The Reticulum stain kit (Abcam, UK) was used for the histological visualization with the guidance of the manual. The assessment of the ALP activity was evaluated by the absorbance at 405 nm. For Alizarin red staining, the cell samples were collected at 21 days and washed with PBS twice, and then fixed with ethanol at 10 min. Following staining was conducted with 0.1% alizarin red solution (Thermo Fisher Scientific, USA) at 10 min. The inverted light microscope was used to observe the staining cell samples.

2.9. Oil red O staining

To further explore the biological functions of miRNA-320a in the adiposyte differentiation of BMSCs, we conducted the Oil red O staining assays. Firstly, the hMSCs were treated with the adipogenic medium, which was composed of low glucose DMEM, 10% FBS, 1 μM/L dexamethasone, 0.5 mM/L 3-Isobutyl-1-methylxanthine (IBMX), 10 μM/L insulin, 200 μM/L indomethacin (Gibco, USA). The LV expression system was also employed to inhibit the expression of miRNA-320a under the control of the empty LV. The cell samples were collected at 21 days and washed with PBS twice, and then fixed with 4% paraformaldehyde (PFA). Following staining was performed using 5 mg/mL Oil red O (dissolved with isopropanol) (Thermo Fisher Scientific, USA) at 30 min. The inverted light microscope was used to observe the staining cell samples.

2.10. Western blotting

Western blotting assays were conducted as previously described [32]. Briefly, the proteins were separated with SDS-PAGE gel, and then the proteins were transferred to the PVDF membrane (Millipore, USA). The protein-contained membranes were incubated with primary antibodies first, including RUNX2 (1:1000, catalog no. sc-390351, Santa Cruz, USA), OSTERIX (1:800, catalog no. sc-393325, Santa Cruz, USA), Osteocalcin (OCN) (1:500, catalog no. sc-390877, Santa Cruz, USA), Osteopontin (OPN) (1:600, catalog no. sc-21742, Santa Cruz, USA), Collagen I (1:1000, catalog no. ab270993, Abcam, USA), adipocyte fatty acid binding protein 2 (AP2) (1:1000, catalog no. 3215, Cell Signaling Technology, USA), CCAAT/enhancer-binding protein α (C/EBPα) (1:600, catalog no. ab128126, Abcam, USA), fatty acid binding protein4 (FABP4) (1:1000, catalog no. 2120, Cell Signaling Technology, USA), peroxisome proliferator-activated receptor γ (PPARγ) (1:1000, catalog no. 2443, Cell Signaling Technology, USA) and Glyceraldehyde 3-phosphate dehydrogenase (GAPDH) (1:5000, catalog no. KM9002T, Tianjin Sungene Biotech Co. ltd, China). Then the membranes were incubated with corresponding secondary antibody (1:10000, BOSTER Biological Technology, China). Finally, image proplus was used to analyze the expression level of these proteins.

2.11. Data analysis and statistics

Statistical analysis of our experimental data was performed by using the SPSS software (version: 22.0). All data were showed with mean ± standard error of the mean (SEM). The Dunnett's T3 Test were performed to compare the difference between two groups and the one-way analysis of variance were used for the rest data. All statistical significance was defined by p value less than 0.05.

3. Results

3.1. Histological changes in TIONFH

To investigate the biopsy of the femoral head of the TIONFH patients and Normal group, the H&E staining assay was performed. The histological images clearly showed the femoral head of the TIONFH patients and NC group. In the NC group, the nuclei of osteocytes and hematopoietic tissue were well stained and in well-proportioned distribution. However, the nuclei of osteocytes were scarce in the femoral head of TIONFH patient, which exhibited obviously aberrant cancellous bone (Fig. 1A).

3.2. Expression of miRNA-320a increased in serum of TIONFH patients

Based on our previous GSE89587 miRNAs expression profile [31], differentially expressed miRNAs between the TIONFH patients and normal controls were screened (Fig. 1B). As shown, total of 11 miRNAs were up-regulated in TIONFH patients, such as miRNA-320a, miRNA-93-5p, and miRNA-25-3p. The rest 18 miRNAs were down-regulated in TIONFH samples in comparison with that of normal samples, including miRNA-4713-5p, miRNA-4674, and miRNA-1914-5p.

Previous studies have revealed that miRNA-320a participated in various disease including cerebral ischemia, several cancers, and lung disease [33–35], but the biological function of miRNA-320a in ONFH remains limited. Hence, the miRNA-320a were selected for the following investigation. The expression profile of miRNA-320a in serum samples was confirmed by qRT-PCR assay, and the results indicated that expression level of miRNA-320a was significantly up-regulated in TIONFH patients (almost 5 times) compared with normal control (p value < 0.01) (Fig. 1C).

3.3. RUNX2 is a target of miRNA-320a

To further elaborate the molecular mechanism of miRNA-320a in the differentiation process of BMSCs, the Target Scan, Pictar, and miRanda database were employed to predicted the potential targets of miRNA-320a. RUNX2 was found to be a target of miRNA-320a. RUNX2 was considered as the pivotal regulator of the osteoblast differentiation [36]. To explore whether RUNX2 was implicated in the development of TIONFH, immunohistochemical staining was performed to detect the expression of RUNX2. In consistent with previous studies [37,38], the expression of RUNX2 was significantly down-regulated in the femoral head tissue of TIONFH patients, and the expression declined almost by half in comparison to the Normal group (p value < 0.01) (Fig. 2A-B). Therefore, we speculate that miRNA-320a may play roles in TIONFH probably by targeting RUNX2. To confirm the binding site of miRNA-320a with RUNX2 3′-UTR, the luciferase report vectors were constructed with wild or mutant RUNX2 3′-UTR segments (RUNX2-3′UTR WT or MUT). The luciferase activity carrying RUNX2-3′UTR WT were significantly weakened by miRNA-320a mimic, but not miRNA-320a NC. Moreover, the luciferase activity carrying RUNX2-3′UTR MUT were not affected by miRNA-320a mimic (Fig. 2C). This result validated the three predicted binding sites of miRNA-320a with RUNX2.

3.4. Overexpression of miRNA-320a inhibits the expression of osteogenesis-related proteins in BMSCs

To investigate the biological functions of miRNA-320a in the osteoblast differentiation, the LV expression system were employed to overexpress miRNA-320a. The expression of miRNA-320a were measured by following qRT-PCR assays. With miRNA-320a contained LV infection, the expression of miRNA-320a were significantly increased and reached the peak at 7 days (Fig. 3A). Firstly, we detected the mRNA expression of RUNX2 in BMSCs after overexpression of miRNA-320a. RUNX2 expression was markedly increased in osteogenic induction of BMSCs at day 5, and the expression was continuously increased in day 7–11, while overexpression of miRNA-320a significantly decreased RUNX2 expression at day 7 (Fig. 3B). Next, we detected the expression levels of osteogenesis-related proteins at day 11. Compared to WT and NC, overexpression of miRNA-320a resulted in obviously decreased

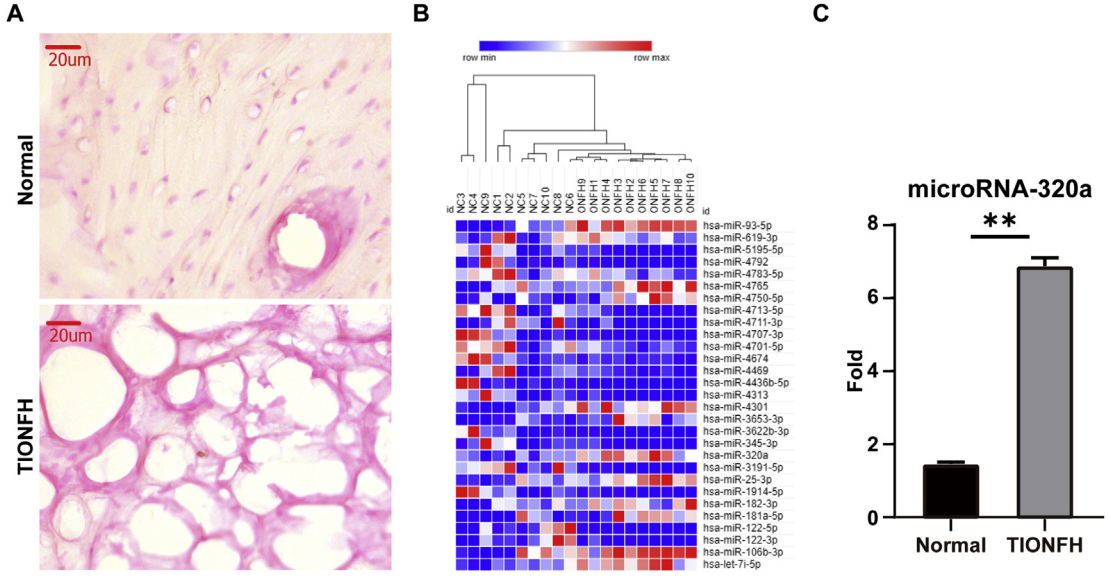

Fig. 1. MiRNAs differentially expressed in TIONFH. A), Representative images of H&E staining in the femoral head of TIONFH and Normal tissue samples. The red bar indicates 20 μm; B) the heat map of miRNAs differentially expressed in between TIONFH and Normal groups. The top panel showed the phylogenetic relationship of all samples and the differentially expressed miRNAs were annotated at the right. Color gradation from blue to red indicated relative elevation in miRNA expression; C), expression of miRNA-320a in serum samples the TIONFH and Normal groups determined by qPCR. ** represented extremely significant difference (p value < 0.01).

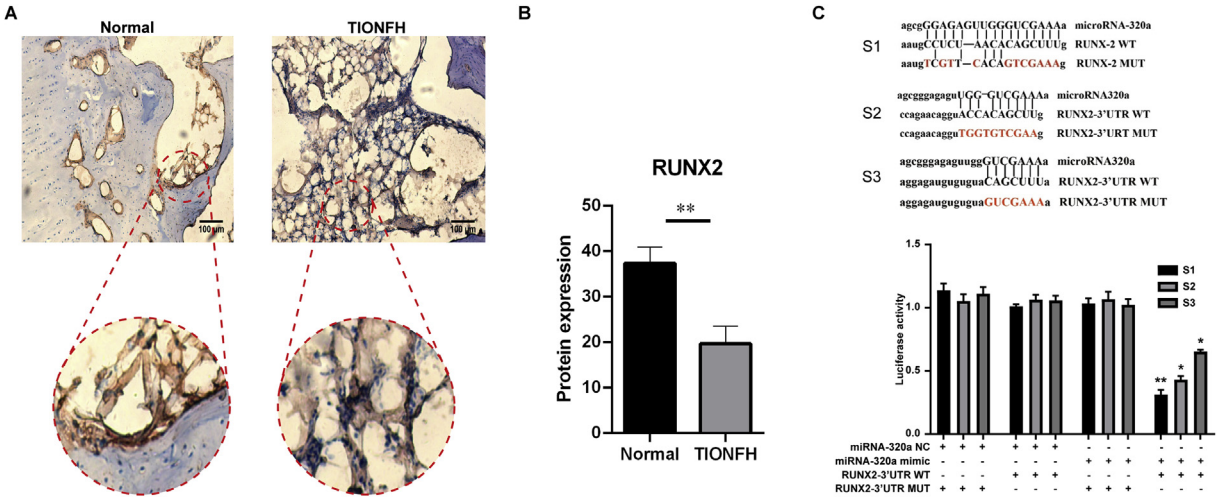

Fig. 2. miRNA-320a directly targets the 3′-UTR of the RUNX2 mRNA. A) Representative images of immunohistochemical staining of RUNX2 in the femoral head of TIONFH and Normal specimens; B) Statistical analysis of RUNX2 expression in the immunohistochemical staining; C) Luciferase reporter carried WT or MUT 3′-UTR of the RUNX2 gene (RUNX2-3′UTR WT and MUT) were transfected into BMSCs. Influence of miRNA-320a on the reporter constructs were detected at 48 h after transfection. * and ** represented significant difference (p value < 0.0.05) and extremely significant difference (p value < 0.01), respectively.

expression of osteogenesis-related proteins including RUNX2, OSTERIX, Collagen I, OCN, and OPN, and the decrease of expression were extremely significant (p value < 0.01) (Fig. 3C-D).

The ALP and Alizarin red staining assays were further employed to validate the inhibition functions of miRNA-320a. Microscopic images clearly showed that the ALP activity was elevated over time in BMSCs and NC BMSCs, but the ALP activity in the miRNA-320a OE BMSCs was not changed (Fig. 4A). In addition, Alizarin red staining results displayed that a crowd of calcium containing osteocytes were observed in the BMSCs and NC BMSCs, but the calcium containing osteocytes were sporadic in the miRNA-320a OE BMSCs (Fig. 4B). Both ALP and Alizarin red staining results implied that the osteogenesis of BMSCs were blocked by the overexpression of miRNA-320a.

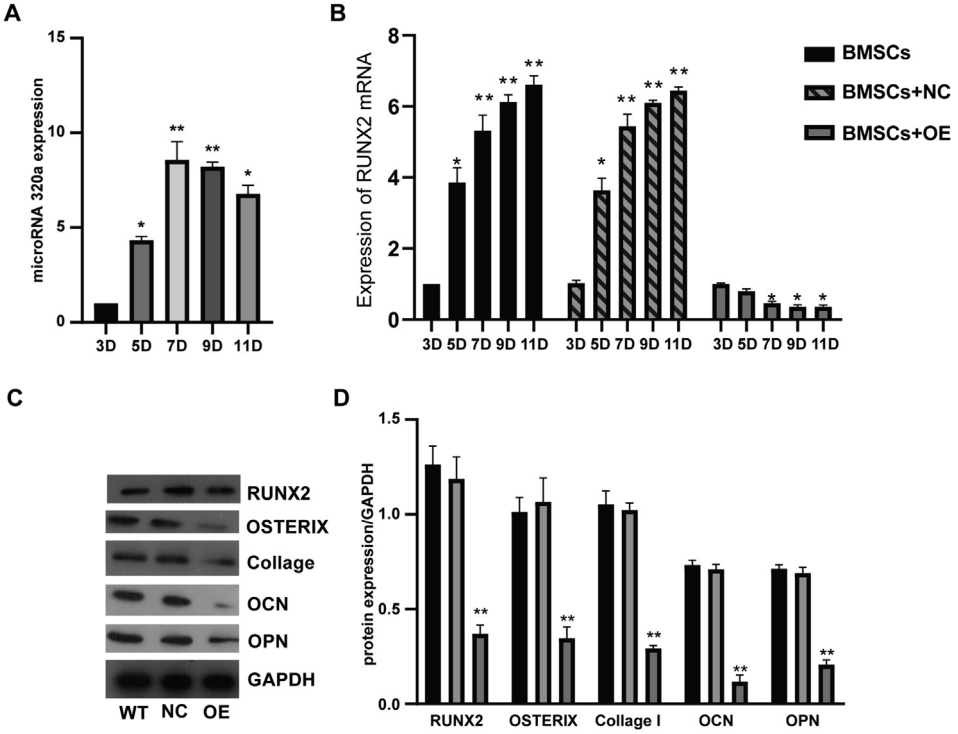

Fig. 3. Overexpression of miRNA-320a inhibits the osteogenesis of BMSCs. A) Expression pattern of miRNA-320a in BMSCs cultured with osteogenic induction medium. B) expression of RUNX2 in osteogenic induction of BMSCs determined by qPCR. C) Western blotting analysis of osteogenesis-relative proteins in BMSCs. GAPDH was acted as the loading control. D) Quantitative analysis of the western blot (n = 3). OE indicated overexpression of miRNA-320a by using the LV expression system and NC indicated the relative negative control. * and ** represented significant difference (p value < 0.05) and extremely significant difference (p value < 0.01), respectively.

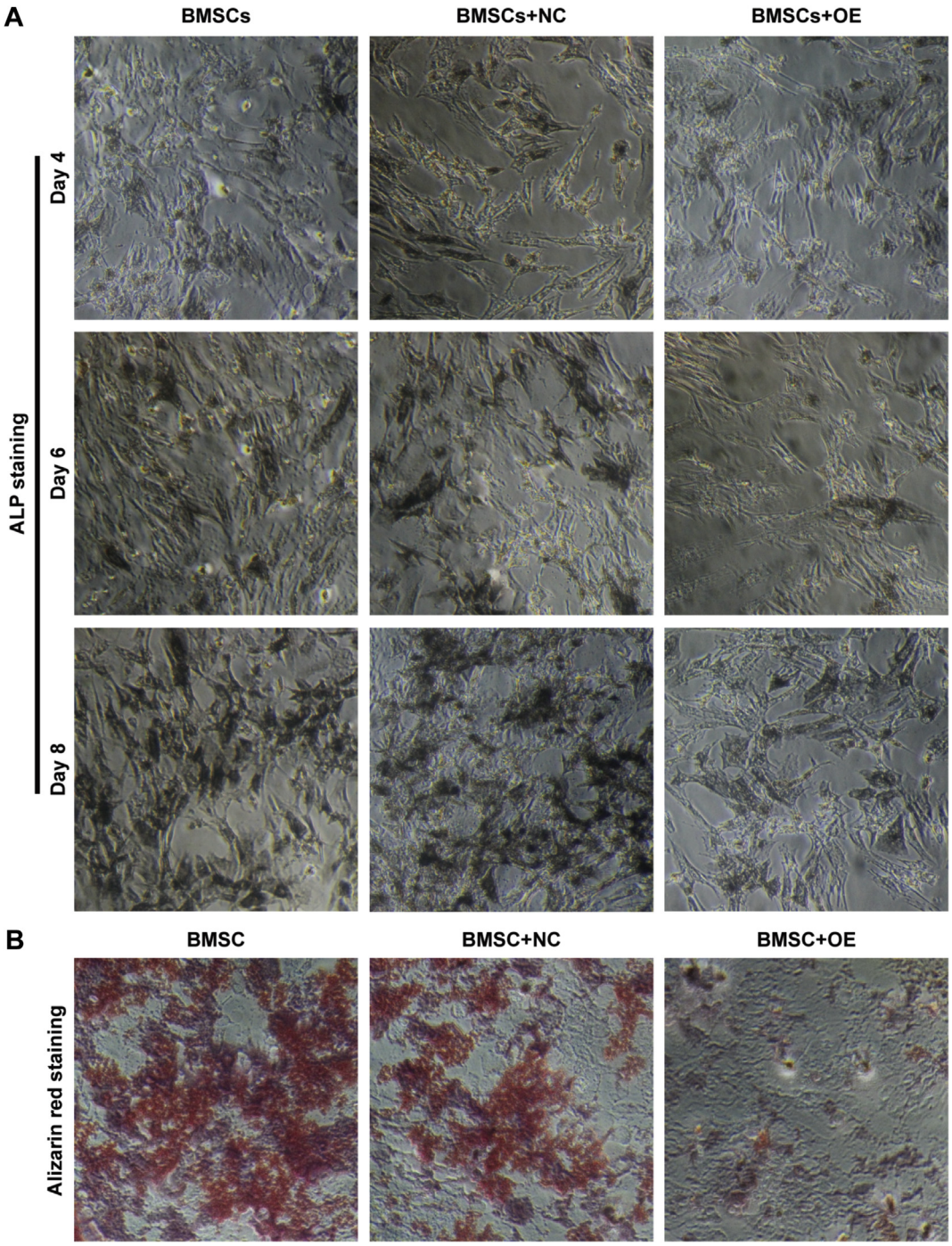

Fig. 4. Overexpression of miRNA-320a inhibits the osteogenesis of BMSCs. A) Microscopic images of ALP staining in BMSCs cultured with osteogenic induction medium. B) Microscopic images of Alizarin red staining in BMCSs. OE indicated overexpression of miRNA-320a by using the LV expression system and NC indicated the relative negative control.

3.5. Inhibition of miRNA-320a reduces the adipogenic differentiation of BMSCs

To further explore the biological functions of miRNA-320a on adipogenic differentiation of BMSCs, the LV expression system-mediated miRNA interference was employed. Following qRT-PCR analysis showed that the expression of miRNA-320a were increased and reached the peak at 9 days with the adipogenic induction, while its expression was significantly suppressed by the LV expression system-mediated miRNA-320a interference (Fig. 5A). Then the expressions of adipogenesis-related proteins were measured by using western blotting assays. With adipogenic induction, apparent expression of AP2, C/EBPα, FABP4, and PPARγ was detected and was significantly suppressed by the inhibitor of miRNA-320a (p value < 0.01) (Fig. 5B-C).

We further performed the Oil Red O staining assays to confirm the function of the miRNA-320a inhibitor. The staining images revealed that a number of well stained lipids were detected in the BMSCs and BMSCs NC, and the stained lipids were infrequent in BMSCs with inhibitor of miRNA-320a (Fig. 5D). This data confirmed the inhibition of miRNA-320a reduces the adipogenesis of BMSCs.

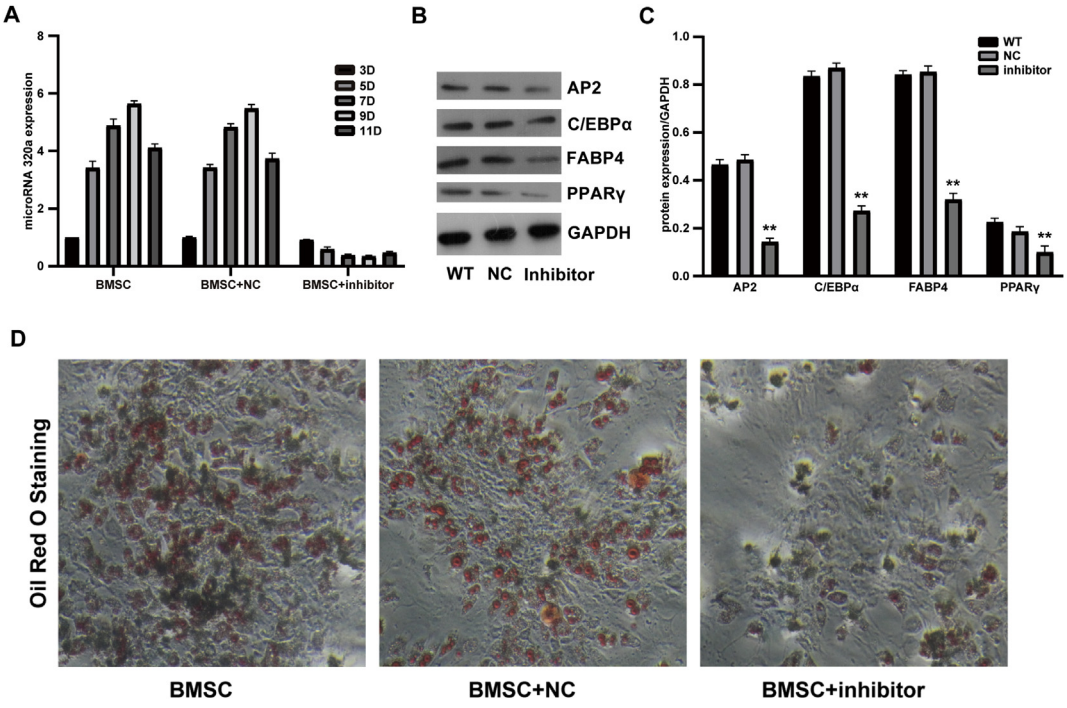

Fig. 5. miRNA-320a promotes adipogenesis of BMSCs. A) Expression profiles of miRNA-320a in BMSCs cultured with adipogenic induction medium. B) Western blotting analysis of adipogenesis-associated proteins in BMSCs. GAPDH was used for the loading control. C) Quantitative analysis of the western blot (n = 3). D) Oil Red O staining of lipids in BMSCs cultured with adipogenic induction medium. Inhibitor indicated the expression of miRNA-320a was inhibited by the LV expression system-mediated miRNA interference and NC indicated the relative negative control. ** represented extremely significant difference (p value < 0.01).

4. Discussion

In the present study, we found that the expression of miRNA-320a was significantly up-regulated while the expression of RUNX2 was significantly down-regulated in the TIONFH patients. Following luciferase report assay determined the miRNA-320a directly binds to the 3′-UTR of RUNX2. H&E staining uncovered the femoral head of TIONFH patient showed aberrant cancellous bone. Moreover, the expressions of osteogenesis associated proteins were blocked by the overexpression of miRNA-320a, including RUNX2, OSTERIX, Collagen I, OCN, and OPN. Subsequent ALP and Alizarin red staining assays revealed that the osteogenesis of BMSCs were inhibited by the overexpression of miRNA-320a. Meanwhile, we demonstrated that the expressions of adipogenesis-related proteins were impeded by the inhibitor of miRNA-320a, such as AP2, C/EBPα, FABP4, and PPARγ. Following Oil Red O staining assays confirmed the inhibition function of the miRNA-320a inhibitor on the adipocyte differentiation of BMSCs. This study is the first identification of the biological functions and molecular mechanisms of miRNA-320a in the differentiation process of BMSCs.

miRNAs generally function as the negative regulator, which binds to the 3′-UTR region of the target mRNA for degrading the binding mRNA or blocking the translation of the target [39]. Previous studies had uncovered that miRNA-320a directly targets to transforming growth factor beta receptor 2 (TGFBR2) and insulin like growth factor 1 receptor (IGF1R) to regulate the fibrotic process of interstitial lung disease [35]. Moreover, Sepramaniam et al. unveiled that miRNA-320a directly targets aquaporins 1 and 4 (AQP1 and AQP4) to modulate the development of cerebral ischemia [33]. miRNA-320a was also identified to facilitate the tumor genesis and progression of epithelial ovarian cancer via targeting ras association domain-containing protein 8 (RASSF8) [34]. Here, miRNA-320a was determined to contribute to the development of ONFH via targeting RUNX2. In summary, miRNA-320a was verified to participate in the development of various diseases by targeting different proteins. Additionally, expression of miRNA-320a was found to be up-regulated in serum sample of TIONFH patients compared with that of normal control. Studies had reported that miRNA-320a had potential predictive value for diagnosis and prognosis in different diseases, such as myelodysplastic syndromes [40], renal ischemia reperfusion [41], and prostate cancer [42]. Therefore, we speculate that expression of miRNA-320a may be a potential diagnostic and prognostic biomarker for TIONFH patients. This should be further confirmed based on clinical data.

Previous studies had dragged the miRNA-320 family (composed of miRNA-320a, miRNA-320b, miRNA-320c, and miRNA-320d) into the regulation of differentiation process in the stem cells [40,43]. miRNA-320c and miRNA-320d were implicated to the differentiation of hematopoietic stem cells [40]. miRNA-320a was identified to regulate the osteogenesis differentiation of BMSCs via targeting homeobox a10 (HOXA10) [43]. In this study, we demonstrated that miRNA-320a inhibited the osteoblast differentiation of BMSCs by directly targeting to RUNX2. Intriguingly, Hoxa10 is a transcription factor which binds to the promoter region of RUNX2 and regulates the expression of RUNX2 [44]. Increasing evidence demonstrated that Runx2 acts as the critical transcription factor which directly participates in the osteoblast differentiation [45]. In addition, Runx2 is a master regulator in osteoblast differentiation process that could regulate the expression of several osteogenesis-associated biomarkers, including OSTERIX, OPN, OCN, and Collagen [46,47]. We also found that the expression of OSTERIX, OPN, OCN, and Collagen I was modulated by miRNA-320a. A number of miRNAs were demonstrated to target RUNX2, however, the miRNAs which directly bind to 3′-UTR of RUNX2 and inhibit its expression are limited [48]. However, three specific binding sites of miRNA-320a in the 3′-UTR of RUNX2 were identified. Our finding implied that miRNA-320a was critical for controlling the expression of RUNX2 and also supported the utmost significance of Runx2 in the osteogenesis of BMSCs.

The abnormally increased bone marrow lipid deposition was reported to be critical for the development of ONFN [11,12]. Increased adipocyte differentiation of BMSCs was implicated in the aberrant elevation of lipid deposition [10]. Most identified miRNAs were reported to attenuate the adipogenesis of BMSCs, like miRNA-27a, miRNA-548d-5p, and miRNA-708 [49–51]. While Hamam et al. demonstrated that overexpression of miRNA-320c promoted adipocytic differentiation of human mesenchymal stem cells, and suggested that miR-320 family could be molecular switch to promote adipocytic differentiation of human mesenchymal stem cells [52]. Consistently, our results indicated that inhibition of miRNA-320a reduced adipogenesis of BMSCs. Hamam et al. and similar findings in our study may imply that overexpression of miRNA-320acontributes to the development of TIONFH via facilitating the lipid deposition. The osteoblast and adipocyte differentiation of BMSCs is balanced under healthy conditions, and disruption of this balance will result in various diseases, like ONFH [53]. A number of researches have proved that miRNAs and their targets were the important regulators in the BMSCs differentiation [46]. For instance, miRNA-130a boosts the osteogenesis of BMSCs via inhibiting the expression of Smad regulatory factors 2 (Smurf2) and inhibiting the adipogenesis of BMSCs by negatively modulating the expression of PPARγ [54]. Here, we demonstrated that miRNA-320a played important roles in regulation of both osteogenesis and adipogenesis of BMSCs. Additionally, Hamam et al. suggested that RUNX2 was the bone fide target for miRNA-320 during adipogenesis [52]. Therefore, we mainly focused on the osteogenesis, and the results showed miRNA-320a mediated osteogenesis by targeting RUNX2. Moreover, three binding sites of miRNA-320a on 3' UTR of RUNX2 were predicted, and the luciferase activity were significantly decreased by miRNA-320a mimic at all three binding sites. These findings indicated that RUNX2 was a prominent target for miRNA-320 family in regulating osteogenesis and adipogenesis.

5. Conclusions

In this study, we identified miRNA-320a and its targets RUNX2 plays important roles in the homeostasis between osteogenesis and adipogenesis in BMSCs. Our results implied miRNA-320a should participate in the development of TIONFH. This study supports miRNAs is critical for the development of TIONFH and helps to elaborate the underlying molecular mechanisms. Our findings also provide a novel target for the diagnosis and therapy of TIONFH.

Ethical approval

This study was in consistent with the relevant provisions of the 1964 Helsinki Declaration and was permitted by the ethics committee of Henan Orthopaedic Hospital.

Informed consent

The informed consent was acquired from all participants.

Availability of data and materials

All data generated or analysed during this study are included in this published article.

Funding

This work was supported by National Science Foundation of China (grant number 81774348 and 81874477); and Science and Technology Project of Henan Province (grant number 212102310365).

Authors' contributions

Conception and design of the research: YZ, NZ, WL; acquisition of data: YD, YL, QY; analysis and interpretation of data: ZJ, ZH, LZ; statistical analysis: QW, WH; obtaining funding: YZ, WL; drafting the manuscript: YZ, NZ; revision of manuscript for important intellectual content: HW, WL. All authors read and approved the final manuscript.

Declaration of competing interest

The authors declare that they have no known competing financial interests or personal relationships that could have appeared to influence the work reported in this paper.

Appendix A. Supplementary data

Supplementary data to this article can be found online at https://doi.org/10.1016/j.reth.2022.03.001.

References

[1] Piuzzi NS, Chahla J, Schrock JB, LaPrade RF, Pascual-Garrido C, Mont MA, et al. Evidence for the use of cell-based therapy for the treatment of osteonecrosis of the femoral head: a systematic review of the literature. J Arthroplasty 2017;32(5):1698–708.
[2] Mont MA, Cherian JJ, Sierra RJ, Jones LC, Lieberman JR. Nontraumatic Osteonecrosis of the femoral head: where do we stand today? A ten-year update. J Bone Joint Surg Am 2015;97(19):1604–27.
[3] Moya-Angeler J, Gianakos AL, Villa JC, Ni A, Lane JM. Current concepts on osteonecrosis of the femoral head. World J Orthop 2015;6(8):590.
[4] Zhao D, Zhang F, Wang B, Liu B, Li L, Kim SY, et al. Guidelines for clinical diagnosis and treatment of osteonecrosis of the femoral head in adults (2019 version). J Orthopaed Trans 2020;21:100–10.
[5] Kuroda Y, Tanaka T, Miyagawa T, Kawai T, Goto K, Tanaka S, et al. Classification of osteonecrosis of the femoral head: who should have surgery? Bone Joint Res 2019;8(10):451–8.
[6] Chen L, Hong G, Fang B, Zhou G, Han X, Guan T, et al. Predicting the collapse of the femoral head due to osteonecrosis: from basic methods to application prospects. J Orthopaed Trans 2017;11:62–72.
[7] Chen S-B, Hu H, Gao Y-S, He H-Y, Jin D-X, Zhang C-Q. Prevalence of clinical anxiety, clinical depression and associated risk factors in Chinese young and middle-aged patients with osteonecrosis of the femoral head. PLos One 2015;10(3):e0120234.
[8] Lespasio MJ, Sultan AA, Piuzzi NS, Khlopas A, Husni ME, Muschler GF, et al. Hip osteoarthritis: a primer. Perm J 2018;22:17–84.
[9] Petek D, Hannouche D, Suva D. Osteonecrosis of the femoral head: pathophysiology and current concepts of treatment. EFORT open reviews 2019;4(3):85–97.
[10] Sheng HH, Zhang GG, Cheung WH, Chan CW, Wang YX, Lee KM, et al. Elevated adipogenesis of marrow mesenchymal stem cells during early steroid-associated osteonecrosis development. J Orthop Surg Res 2007;2:15.
[11] Wang G-J, Sweet D, Reger SI, Thompson RC. Fat-cell changes as a mechanism of avascular necrosis of the femoral head in cortisone-treated rabbits. J Bone Joint Surg Am 1977;59(6):729–35.
[12] Wang Y, Li Y, Mao K, Li J, Cui Q, Wang G-J, et al. Alcohol-induced adipogenesis in bone and marrow: a possible mechanism for osteonecrosis. Clin Orthop Relat Res 2003;410:213–24.
[13] Cooke PS, AJ Naaz. Role of estrogens in adipocyte development and function. Exp Biol Med 2004;229(11):1127–35.
[14] Cup Q, Wang G-J, G Balian. Pluripotential marrow cells produce adipocytes when transplanted into steroid-treated mice. Connect Tissue Res 2000;41(1):45–56.
[15] Tomlinson JJ, Boudreau A, Wu D, Atlas E, Haché RJG. Modulation of early human preadipocyte differentiation by glucocorticoids. Endocrinology 2006;147(11):5284–93.
[16] Ng KS, Kuncewicz TM, Karp JM. Beyond hit-and-run: stem cells leave a lasting memory. Cell Metab 2015;22(4):541–3.
[17] Lee H, Min SK, Park JB. Effects of demographic factors on adipogenic and chondrogenic differentiation in bone marrow-derived stem cells. Exp Ther Med 2019;17(5):3548–54.
[18] Yang Z, Shah K, Khodadadi-Jamayran A, Jiang H. Dpy30 is critical for maintaining the identity and function of adult hematopoietic stem cells. J Exp Med 2016;213(11):2349–64.
[19] Su T, Xiao Y, Xiao Y, Guo Q, Li C, Huang Y, et al. Bone marrow mesenchymal stem cells-derived exosomal MiR-29b-3p regulates aging-associated insulin resistance. ACS Nano 2019;13(2):2450–62.

[20] Houdek MT, Wyles CC, Packard BD, Terzic A, Behfar A, RJ Sierra. Decreased osteogenic activity of mesenchymal stem cells in patients with corticosteroid-induced osteonecrosis of the femoral head. J Arthroplasty 2016;31(4):893–8.
[21] Yeh C-H, Chang J-K, Ho M-L, Chen C-H, Wang G-J. Different differentiation of stroma cells from patients with osteonecrosis: a pilot study. Clin Orthop Relat Res 2009;467(8):2159–67.
[22] Balla B, Pintér C, Kósa JP, Podani J, Takács I, Nagy Z, et al. Gene expression changes in femoral head necrosis of human bone tissue. Dis Markers 2011;31(1):25–32.
[23] Xiang S, Li Z, Weng X. Changed cellular functions and aberrantly expressed miRNAs and circRNAs in bone marrow stem cells in osteonecrosis of the femoral head. Int J Mol Med 2020;45(3):805–15.
[24] Wu X, Zhang Y, Guo X, Xu H, Xu Z, Duan D, et al. Identification of differentially expressed microRNAs involved in non-traumatic osteonecrosis through microRNA expression profiling. Gene 2015;565(1):22–9.
[25] Bartel DP. Metazoan MicroRNAs. Cell 2018;173(1):20–51.
[26] Bartel DP. MicroRNAs: target recognition and regulatory functions. Cell 2009;136(2):215–33.
[27] Wang XJ, Reyes JL, Chua NH, Gaasterland T. Prediction and identification of Arabidopsis thaliana microRNAs and their mRNA targets. Genome Biol 2004;5(9):R65.
[28] Zhao R, Li Y, Lin Z, Wan J, Xu C, Zeng Y, et al. miR-199b-5p modulates BMSC osteogenesis via suppressing GSK-3β/β-catenin signaling pathway. Biochem Biophys Res Commun 2016;477(4):749–54.
[29] Li T, Li H, Wang Y, Li T, Fan J, Xiao K, et al. microRNA-23a inhibits osteogenic differentiation of human bone marrow-derived mesenchymal stem cells by targeting LRP5. Int J Biochem Cell Biol 2016;72:55–62.
[30] Tang Y, Zhang L, Tu T, Li Y, Murray D, Tu Q, et al. MicroRNA-99a is a novel regulator of KDM6B-mediated osteogenic differentiation of BMSCs. J Cell Mol Med 2018;22(4):2162–76.
[31] Zhang Y, Wei QS, Ding WB, Zhang LL, Wang HC, Zhu YJ, et al. Increased microRNA-93-5p inhibits osteogenic differentiation by targeting bone morphogenetic protein-2. PLoS One 2017;12(8):e0182678.
[32] Li H, Xie H, Liu W, Hu R, Huang B, Tan YF, et al. A novel microRNA targeting HDAC5 regulates osteoblast differentiation in mice and contributes to primary osteoporosis in humans. J Clin Invest 2009;119(12):3666–77.
[33] Sepramaniam S, Armugam A, Lim KY, Karolina DS, Swaminathan P, Tan JR, et al. MicroRNA 320a functions as a novel endogenous modulator of aquaporins 1 and 4 as well as a potential therapeutic target in cerebral ischemia. J Biol Chem 2010;285(38):29223–30.
[34] Zhang L, Chen H, He F, Zhang S, Li A, Zhang A, et al. MicroRNA-320a promotes epithelial ovarian cancer cell proliferation and invasion by targeting RASSF8. Front Oncol 2021;11(200).
[35] Li Y, Huang J, Hu C, Zhou J, Xu D, Hou Y, et al. MicroRNA-320a: an important regulator in the fibrotic process in interstitial lung disease of systemic sclerosis. Arthritis Res Ther 2021;23(1):21.
[36] Wysokinski D, Pawlowska E, Blasiak J. RUNX2: a master bone growth regulator that may be involved in the DNA damage response. DNA Cell Biol 2015;34(5):305–15.
[37] Zhu W, Guo M, Yang W, Tang M, Chen T, Gan D, et al. CD41-deficient exosomes from non-traumatic femoral head necrosis tissues impair osteogenic differentiation and migration of mesenchymal stem cells. Cell Death Dis 2020;11(4):293.
[38] Huang L, Wang Y, Jiang Y, Wu Y, Hu C, Ouyang H. High levels of GSK-3β signalling reduce osteogenic differentiation of stem cells in osteonecrosis of femoral head. J Biochem 2018;163(3):243–51.
[39] DP Bartel. MicroRNAs: genomics, biogenesis, mechanism, and function. Cell 2004;116(2):281–97.
[40] Wan C, Wen J, Liang X, Xie Q, Wu W, Wu M, et al. Identification of miR-320 family members as potential diagnostic and prognostic biomarkers in myelodysplastic syndromes. Sci Rep 2021;11(1):183.
[41] Güçlü A, Koçak C, Koçak FE, Akçılar R, Dodurga Y, Akçılar A, et al. Micro RNA-320 as a novel potential biomarker in renal ischemia reperfusion. Ren Fail 2016;38(9):1468–75.
[42] Lieb V, Weigelt K, Scheinost L, Fischer K, Greither T, Marcou M, et al. Serum levels of miR-320 family members are associated with clinical parameters and diagnosis in prostate cancer patients. Oncotarget 2018;9(12):10402–16.
[43] Huang J, Meng Y, Liu Y, Chen Y, Yang H, Chen D, et al. MicroRNA-320a regulates the osteogenic differentiation of human bone marrow-derived mesenchymal stem cells by targeting HOXA10. Cell Physiol Biochem 2016;38(1):40–8.
[44] Hassan MQ, Tare R, Lee SH, Mandeville M, Weiner B, Montecino M, et al. HOXA10 controls osteoblastogenesis by directly activating bone regulatory and phenotypic genes. Mol Cell Biol 2007;27(9):3337–52.
[45] Sun M, Chi G, Li P, Lv S, Xu J, Xu Z, et al. Effects of matrix stiffness on the morphology, adhesion, proliferation and osteogenic differentiation of mesenchymal stem cells. Int J Med Sci 2018;15(3):257–68.
[46] Yin N, Zhu L, Ding L, Yuan J, Du L, Pan M, et al. MiR-135-5p promotes osteoblast differentiation by targeting HIF1AN in MC3T3-E1 cells. Cell Mol Biol Lett 2019;24:51.
[47] Teplyuk NM, Galindo M, Teplyuk VI, Pratap J, Young DW, Lapointe D, et al. Runx2 regulates G protein-coupled signaling pathways to control growth of osteoblast progenitors. J Biol Chem 2008;283(41):27585–97.
[48] Narayanan A, Srinaath N, Rohini M, Selvamurugan N. Regulation of Runx2 by MicroRNAs in osteoblast differentiation. Life Sci 2019;232:116676.
[49] Gu C, Xu Y, Zhang S, Guan H, Song S, Wang X, et al. miR-27a attenuates adipogenesis and promotes osteogenesis in steroid-induced rat BMSCs by targeting PPARγ and GREM1. Sci Rep 2016;6(1):1–12.
[50] Sun J, Wang Y, Li Y, Zhao G. Downregulation of PPARγ by miR-548d-5p suppresses the adipogenic differentiation of human bone marrow mesenchymal stem cells and enhances their osteogenic potential. J Transl Med 2014;12(1):1–8.
[51] Hao C, Yang S, Xu W, Shen JK, Ye S, Liu X, et al. MiR-708 promotes steroid-induced osteonecrosis of femoral head, suppresses osteogenic differentiation by targeting SMAD3. Sci Rep 2016;6(1):1–13.
[52] Hamam D, Ali D, Vishnubalaji R, Hamam R, Al-Nbaheen M, Chen L, et al. microRNA-320/RUNX2 axis regulates adipocytic differentiation of human mesenchymal (skeletal) stem cells. Cell Death Dis 2014;5(10):e1499.
[53] Kang H, Hata A. The role of microRNAs in cell fate determination of mesenchymal stem cells: balancing adipogenesis and osteogenesis. BMB Rep 2015;48(6):319–23.
[54] Lin Z, He H, Wang M, Liang J. MicroRNA-130a controls bone marrow mesenchymal stem cell differentiation towards the osteoblastic and adipogenic fate. Cell Prolif 2019;52(6):e12688.